symmetry

MDPI

Article

Evaluation of the Dynamic Impact of a Passing Vehicle on a Bridge Deck Due to a Damaged Expansion Joint

Jing Gao *, Xintao Zhang and Jiayan Lei

School of Architecture and Civil Engineering, Xiamen University, Xiamen 361005, China; 25320211152312@stu.xmu.edu.cn (X.Z.); leijiayan7836@163.com (J.L.)
* Correspondence: gaojing@xmu.edu.cn

Abstract: When a vehicle passes over a bridge, it may jump on the bridge due to a damaged expansion joint. The sudden jump induces a heavy dynamic impact on the bridge and therefore damages the bridge deck and girder. The traditional dynamic amplification factor defined by the current bridge design code shows the amplification of the static effects on the bridge. However, it only concerns the stable moving load induced by the vehicle. The sudden vehicle impact due to a damaged expansion joint sometimes exceeds the allowable design load, so it is important to evaluate the dynamic impact in practice. In fact, the dynamic impact can be approximately considered as a contact force between a damped harmonic oscillator and a beam due to the bilateral symmetry of the vehicle; therefore, a model-based approach using the bridge midspan acceleration is proposed in this study to approximately evaluate the impact force, where it is assumed as an exponentially damped sine function. This is a typical parametric model-based inverse problem. The conjugate direction method is used to determine the unknown parameters and the initial values are determined by a simple global search method. Since only five parameters are included, the proposed method is simpler than the conventional basis function-based methods. Numerical simulations were conducted to validate the proposed method. Generally, the proposed method performs well to identify the dynamic impact. In particular, the displacement measured directly from the bridge is preferred since the displacement obtained from the acceleration has numerical errors; the measurement noise in the range of 1% to 5% shows a slight influence on the proposed method; and the error of frequencies and mode shapes greatly affects the proposed method, especially for the maximum force.

Keywords: dynamic impact; damaged expansion joint; vehicle bridge interaction; load identification

Citation: Gao, J.; Zhang, X.; Lei, J. Evaluation of the Dynamic Impact of a Passing Vehicle on a Bridge Deck Due to a Damaged Expansion Joint. *Symmetry* **2022**, *14*, 813. https://doi.org/10.3390/sym14040813

Academic Editors: Yang Yang, You Dong, Yao Zhang and Tianyu Xie

Received: 18 March 2022
Accepted: 12 April 2022
Published: 14 April 2022

1. Introduction

Expansion joints are usually used to connect bridge girders. However, the expansion joint is always subjected to impact loads since the surface is uneven. The expansion joint can be damaged easily and induce more significant vehicle impact on the bridge deck and girders. The sudden heavy shear force may further result in shear cracks in the girders. Therefore, it is important to evaluate heavy impacts induced by damaged expansion joints.

The dynamic impact factor and dynamic amplification factor are usually used in bridge design codes [1–3] to describe the dynamic effect of vehicles on bridges, and generally consider a stable moving load. Cai et al. [4] and Shi et al. [5] calculated the vehicle-induced dynamic response of short span slab bridges through a 3D finite element model of a vehicle–bridge interaction system, and they observed that the fault at the end of the approach slab resulted in significantly large dynamic responses. Deng et al. [6] investigated the vehicle impact on the deck slab of concrete box girder bridges due to damaged expansion joints and proposed a local impact factor to compare with the conventional impact factor. Ding et al. [7,8] conducted finite element simulations to analyze the dynamic load of the vehicle, and found that the impact factor sometimes exceeded the allowable design load when the vehicle passed over the bumps of the bridge head. Xie et al. [9] carried out a

field experiment to measure the dynamic behavior of steel box girder bridges subjected to vehicle-induced impact and concluded that vibration near the expansion joint was more significant. In addition, research [10–12] has also been conducted to investigate the dynamic amplification of impacts on bridge columns. The above-mentioned investigations all focused on forward problems, which means that the dynamic impact is known, and the effect of the impact on the bridge is investigated accordingly. In fact, the vehicle impact force induces shear cracks on the bridge girder near bridge piers, but is difficult to measure in practice; therefore, it is important to propose a method to evaluate the vehicle impact.

Identification of load based on structural vibration data has been well investigated in recent decades [13,14]. Usually there are two approaches: one uses updated finite element (FE) models and the other is based on measured modal parameters. For the first method, a FE model is constructed first and then the calculated dynamic responses are used to compare with measurements; the FE model is then updated according to the error between the measurement and the calculation. Finally, not only the impact force, but also the parameters of the vehicle, can be identified through this method. Law et al. [15] proposed a regularization method to identify the moving force, which can reduce the significant fluctuations at the beginning and end of the time history. Au et al. [16] used advanced genetic algorithms to identify the vehicle parameters used in the FE model. Deng and Cai [17] identified the parameters of vehicles passing over more complex bridges using a modal superposition method which simplified the construction of the FE model. Vosoughi and Anjabin [18] proposed a hybrid method to identify the dynamic moving load on composite beams, which also requires the FE model. However, constructing an accurate FE model is usually difficult in practice, especially for these large-scale structures. For the second method, only modal parameters that can be easily measured are required and the force can be identified by solving regularization problems. Considering that the measurement is polluted by noise, Gunawan [19] proposed the regularized Wiener filter method to reconstruct the impact force. Li and Lu [20] developed a constrained optimization scheme to localize the impact force and then identify its time history. Gupta and Dhingra [21] tried to estimate the dynamic force by using the acceleration obtained at optimal locations. However, an ill-conditioned matrix and noise are usually found in these conventional time domain methods; therefore, the basis function method is attractive. Several basis functions have been applied to force identification, in which the force is de-composited by these basis functions. Liu et al. [22] approximated the distributed force by using a set of triangle functions. Gunawan [23–25] reconstructed the impact force using harmonic functions, quadratic spline functions, and B spline functions as the basis function, and discussed regularization of the ill-posed problem. Qiao et al. [26] proposed a method based on B spline scaling functions to identify the force; in particular, they discussed an algorithm to determine the number of basis functions required to eliminate underestimation and overestimation. Li et al. [27] decomposed the impact force and sinusoidal force into a series of Daubechies wavelets, and the proposed method showed better results than the frequency domain method in experimental examples. Xu and Ou [28] presented a moving least square method based on the virtual work principle, where the impact force in a short period was approximated by polynomial functions. Pourzeynali et al. [29] attempted to identify the moving load on bridge structures using the explicit form of the Newmark-β method, and validated the approach by both numerical and experimental studies. Wang et al. [30] identified both static and dynamic loads applied on a bridge using acceleration and inclination responses. Generally, for these methods using basis functions, the basis function should be carefully selected and the number of orders to be used should be carefully determined. Recently, more advanced non-parametric load identification approaches have been developed based on artificial intelligence algorithms [31,32]; however, these usually require a large amount of testing data for training.

Because the dynamic impact can be approximately simplified as a contact force between a damped harmonic oscillator and a beam due to the vehicle's bilateral symmetry, a model-based approach is proposed in this study to approximate the impact force, where it

is assumed as an exponentially damped sine function; this is also a basis function that is specific to this problem. This is based on the observation from previous studies that the shape of the impact force time history is similar to the shape of this function [4,7–9,33,34]. Then, the impact force identification is converted to a typical optimization problem to determine the parameters used in the function. Although this method is not suitable for general force identification, it is more reliable and noise-robust than other methods for this specific problem because the force model is quite close to the true one. Moreover, it is simpler than the general function-based method because it has fewer parameters. In fact, quick and accurate identification of heavy impacts due to a vehicle passing the damaged expansion joint is important to ensure the structure's safety, and may prevent the sudden failure of the bridge from shear failure.

This study is organized as follows: Section 2 presents the relevant theory, including the construction of the exponentially damped sine function and the optimization model for impact approximation. Section 3 shows numerical examples to validate the proposed method and investigates the influence of measurement noise and modal error. Finally, conclusions and discussions are presented in Section 4.

2. Model-Based Impact Identification

The general equation of linear vibration of a continuous system can be written as:

$$\mathbf{M}\ddot{\mathbf{X}} + \mathbf{C}\dot{\mathbf{X}} + \mathbf{K}\mathbf{X} = \mathbf{F} \tag{1}$$

where **M** is the mass matrix, **C** is the damping matrix, **K** is the stiffness matrix, **X** is the displacement vector, and **F** is the applied force vector [16]. Using the modal superposition method, the ith modal equation of the structure can be obtained as [20]:

$$m_i\ddot{q}_i + 2\xi_i\omega_i\dot{q}_i + \omega_i^2 q_i = Q_i(t) \tag{2}$$

$$Q_i(t) = \int_\Omega \phi_i f(t) \tag{3}$$

where m_i, ξ_i, ω_i, and ϕ_i are the ith modal mass, damping ratio, natural frequency, and mode shape, respectively. $Q_i(t)$ is the ith modal force. q_i is the ith order modal response and can be obtained as the following convolution:

$$q_i(t) = Q_i(t) \otimes h_i(t) \tag{4}$$

where $h_i(t)$ is the ith impulse response function:

$$h_i(t) = \frac{1}{m_i\omega_i\sqrt{1-\xi_i^2}} e^{-\xi_i\omega_i t} \sin\left(\sqrt{1-\xi_i^2}\omega_i t\right) \tag{5}$$

The ith modal force $Q_i(t)$ is simplified as [20]:

$$Q_i(t) = \phi_i\left(s_f\right) f(t) \tag{6}$$

where s_f is the location of the contact point and is time-varying. In this study, the vehicle velocity is considered as a constant, v, in this short time duration and, therefore, $s_f = vt$. s_r is the location of the sensor and it is at the midspan in this study.

Then the displacement response at s_r is obtained by the modal superposition method:

$$x(s_r,\ t) = \sum_i \phi_i(s_r) q_i(t) = \sum_i \phi_i(s_r)\phi_i\left(s_f\right) f(t) \otimes h_i(t) \tag{7}$$

Furthermore, Equation (7) can be written in the discrete form:

$$\begin{aligned}\mathbf{x}(s_r,\ t) &= \begin{pmatrix} x(s_r,\ \Delta t) \\ x(s_r,\ 2\Delta t) \\ \vdots \\ x(s_r, N\ \Delta t) \end{pmatrix} \\ = \sum_i \phi_i(s_r) \begin{pmatrix} h_i(\Delta t) & & \\ \vdots & \ddots & \\ h_i(N\Delta t) & \dots & h_i(\Delta t) \end{pmatrix} &\begin{pmatrix} \phi_i(0)f(0) \\ \vdots \\ \phi_i(v(N-1)\Delta t)f((N-1)\Delta t) \end{pmatrix} \Delta t \\ &= \sum_i \phi_i(s_r)\mathbf{H}_i \mathrm{f}_i \Delta t\end{aligned} \tag{8}$$

where Δt is the sampling interval, N is the number of sampling points.

Then, the vehicle velocity, v, and the impact force, $\mathbf{f} = (f(0), f(\Delta t), \cdots, f((N-1)\Delta t))^{\mathrm{T}}$, can be obtained by solving the following optimization problem:

$$(v, \mathbf{f}) = \min_{v,\mathbf{f}} \|\mathbf{x}(s_r,\ t) - \mathbf{u}(s_r,\ t)\| \tag{9}$$

where $\mathbf{u}(s_r,\ t)$ is the measured displacement at s_r.

In this study, the impact force is modeled as an exponentially damped sine function, which can be seen in Figure 1. This is because, in the previous studies [4,7–9], the impact induced by a vehicle looks like an exponentially damped sine function. The impact force can be recognized as:

$$f(t) = G + Ae^{-\omega\xi t} \sin\left(\omega t - \frac{\pi}{2}\right) \tag{10}$$

where G, A, ω, and ξ are to-be-determined parameters.

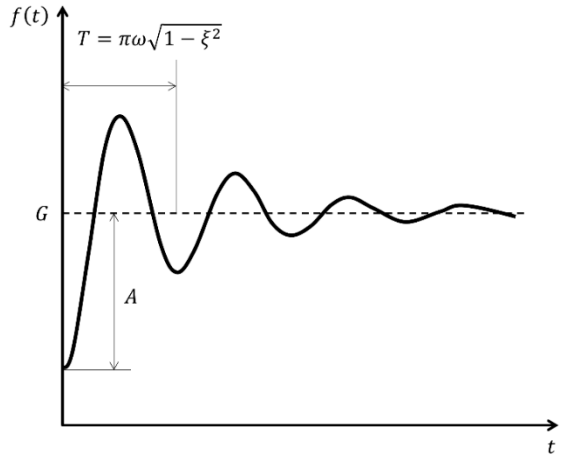

Figure 1. Illustration of an exponentially damped sine function.

Then, the problem should be reorganized as:

$$(v, G, A, \omega, \xi) = \min_{v,G,A,\omega,\xi} \|\mathbf{x}(s_r,\ t) - \mathbf{u}(s_r,\ t)\| \tag{11}$$

The above optimization problem can be solved by the conjugate direction method [35]. This method is suitable for the specific problem because it does not require calculating derivatives. The procedure for implementing this algorithm is simply listed as follows, and is also shown in Figure 2. For simplicity, only two variables, A and ω, are considered in the illustration.

(1) Set up an initial point $\left(\boldsymbol{A}^{(\mathbf{0})}, \boldsymbol{\omega}^{(\mathbf{0})}\right)$ and two initial conjugate vectors $\mathbf{S}_{\mathbf{1}}^{(\mathbf{0})}$, $\mathbf{S}_{\mathbf{2}}^{(\mathbf{0})}$, which are selected as unit vectors in this study.

(2) Search for the point $\left(A^{(0)}, \omega^{(0)}\right) + \lambda^{(0)}\mathbf{S}_1^{(0)}$ to obtain the minimum value of $\|\mathbf{x}(s_r,\ t) - \mathbf{u}(s_r,\ t)\|$ along the first conjugate direction $\mathbf{S}_1^{(0)}$, then search for the point $\left(A^{(0)}, \omega^{(0)}\right) + \lambda^{(0)}\mathbf{S}_1^{(0)} + \eta^{(0)}\mathbf{S}_2^{(0)}$ to obtain the minimum value of $\|\mathbf{x}(s_r,\ t) - \mathbf{u}(s_r,\ t)\|$ along the second conjugate direction $\mathbf{S}_2^{(0)}$.

(3) Search for the next iteration point $\left(A^{(1)}, \omega^{(1)}\right)$ to obtain the minimum value of $\|\mathbf{x}(s_r,\ t) - \mathbf{u}(s_r,\ t)\|$ along the direction $\lambda^{(0)}\mathbf{S}_1^{(0)} + \eta^{(0)}\mathbf{S}_2^{(0)}$.

(4) Set the two new conjugate vectors as: $\mathbf{S}_1^{(1)} = \mathbf{S}_2^{(0)}$, $\mathbf{S}_2^{(1)} = \lambda^{(0)}\mathbf{S}_1^{(0)} + \eta^{(0)}\mathbf{S}_2^{(0)}$.

(5) Repeat Steps (2)–(4).

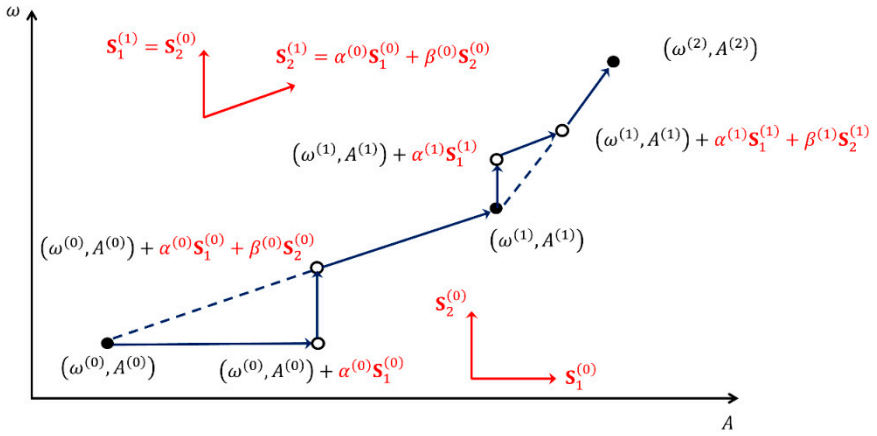

Figure 2. Illustration of the conjugate direction method.

After n iterations, the procedure converges to the final point $\left(A^{(n)}, \omega^{(n)}\right)$ if the following criterion is satisfied:

$$\|\left(A^{(n)}, \omega^{(n)}\right) - \left(A^{(n-1)}, \omega^{(n-1)}\right)\| \leq \delta \tag{12}$$

where δ is the pre-determined threshold. It is set as 1×10^{-6} in this study [17].

However, it should be noted that the result is quite sensitive to the initial values. Therefore, the initial values should be selected carefully. In fact, G is related to the weight of the vehicle, A is related to the value of dropping height, and ω and ξ are related to the frequency and damping of the vehicle, respectively. Considering that v is the vehicle velocity, all five parameters have physical meanings and, therefore, they should be in a reasonable range.

$$v \in [v_l, v_u] \tag{13a}$$

$$G \in [G_l, G_u] \tag{13b}$$

$$A \in [A_l, A_u] \tag{13c}$$

$$\omega \in [\omega_l, \omega_u] \tag{13d}$$

$$\xi \in [\xi_l, \xi_u] \tag{13e}$$

where v_l and v_u are the lower and upper bounds of the vehicle velocity, and are set as 1 and 40 m/s, respectively, in this study; G_l and G_u are set as 980 and 294,000 N because the vehicle is usually in the range of 100 to 30,000 kg; A_l and A_u are set as 0 and $G/2$, respectively, by considering that the vehicle does not separate from the bridge; ω_l and ω_u are set as 12 and 65 rad/s, respectively, because the vehicle frequency is usually between 2 and 10 Hz; and ξ_l and ξ_u are set as 0.001 and 0.1, respectively, since the damping is roughly in the range of 0.1% to 10%.

A two-step algorithm is proposed in this study to determine the initial values. For the first step, G is assumed as 980 N, which is the lower bound, and A is assumed as 490 N, which is the upper bound, when G is determined. Then, the initial values of v, ω, and ξ can be determined by solving the following problem:

$$(v,\omega,\xi)=\min_{v,\omega,\xi}\left(1-\frac{\mathbf{x}^{\mathrm{T}}(s_r,\,t)\mathbf{u}(s_r,\,t)}{\|\mathbf{x}(s_r,\,t)\|\|\mathbf{u}(s_r,\,t)\|}\right)\text{subject to}\begin{cases} v\in\left(v_l,v_l+\frac{v_h-v_l}{n_v-1},v_l+2\frac{v_h-v_l}{n_v-1},\cdots,v_h\right)\\ \omega\in\left(\omega_l,\omega_l+\frac{\omega_h-\omega_l}{n_\omega-1},\omega_l+2\frac{\omega_h-\omega_l}{n_\omega-1},\cdots,\omega_h\right)\\ \xi\in\left(\xi_l,\xi_l+\frac{\xi_h-\xi_l}{n_\xi-1},\xi_l+2\frac{\xi_h-\xi_l}{n_\xi-1},\cdots,\xi_h\right)\end{cases} \tag{14}$$

where n_v, n_ω, n_ξ are integers. In fact, this step is just to find v, ω, and ξ among the $n_v\times n_\omega\times n_\xi$ values to ensure the shapes of the estimated and measured displacements are close. This is because the two shapes are more similar the closer the value of $\frac{\mathbf{x}^{\mathrm{T}}(s_r,\,t)\mathbf{u}(s_r,\,t)}{\|\mathbf{x}(s_r,\,t)\|\|\mathbf{u}(s_r,\,t)\|}$ is to 1. In this study, n_v, n_ω, and n_ξ are 30, 30, and 10, respectively.

Then, in the second step, based on the determined values of v, ω, and ξ, the initial values of G and A can be obtained by solving the following problem:

$$(G,A)=\min_{G,A}\|\mathbf{x}(s_r,\,t)-\mathbf{u}(s_r,\,t)\|$$
$$\text{subject to}\begin{cases} G\in\left(G_l,G_l+\frac{G_h-G_l}{n_G-1},G_l+2\frac{G_h-G}{n_G-1},\cdots,G_h\right)\\ A\in\left(A_l,v_l+\frac{A_h-A_l}{n_A-1},A_l+2\frac{A_h-A}{n_A-1},\cdots,A_h\right)\end{cases} \tag{15}$$

where n_G and n_A, are integers. This step ensures the estimated and measured displacements are approximate. In this study, n_G and n_A are 1000 and 10, respectively.

When the initial values of G, A, v, ω, and ξ are determined, the optimization problem (Equation (11)) can be effectively solved by the conjugate direction method. Figure 3 shows the flowchart of the proposed method. First, modal analysis of the bridge should be conducted to extract the modal frequencies and mode shapes of the bridge. Then, once the displacement of the bridge midspan is obtained, either by direct measurement or integration of acceleration, the conjugate direction method can be adopted to evaluate the unknown parameters. Finally, the time history of the dynamic impact can be obtained accordingly.

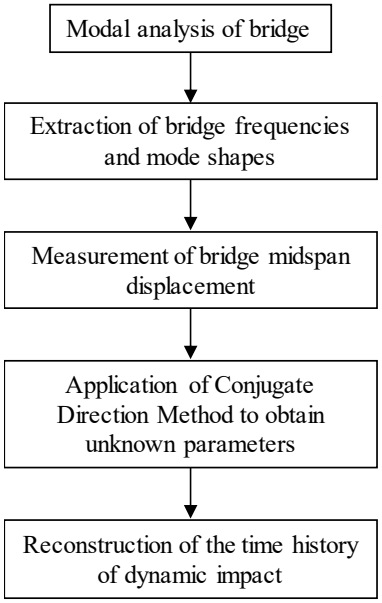

Figure 3. Flowchart of the proposed method.

3. Numerical Simulation

The FE model was constructed using ABAQUS (v6.14). It should be noted that other general purpose FE software, such as ANSYS, can also be used to construct the FE model. An ordinary passenger vehicle and a typical short span girder bridge similar to those in Refs. [3,5,13] were selected. The model is shown in Figure 4. The vehicle is modeled as a mass-spring system with a velocity of v because of the bilateral symmetry of the vehicle, and the bridge is modeled as a simply supported Euler beam. The damaged expansion joint is approximately modeled as a height gap of Δ. The properties are as follows: the length of the bridge is 25 m; the elastic modulus and density of the concrete are 27.5 GPa and 2400 kg/m^3, respectively; the cross-sectional area and moment of inertia are 2 m^2 and 0.12 m^4, respectively; and the mass, stiffness, and damping ratio of the vehicle are 1200 kg, 500 kN/m, and 3%, respectively. The sampling frequency is 100 Hz. Six different cases are considered: H05V10, H05V15, H05V20, H10V10, H10V15, and H10V20. H05 and H10 indicate Δ is 5 and 10 mm, and V10, V15, and V20 indicate that the vehicle velocity is 10, 15, and 20 m/s, respectively. In this study, the first five modes are used. It should be noted that the method does not depend on the material properties of the bridge or the vehicle; therefore, the effect of the material properties of the bridge and vehicle on the proposed method can be neglected, and this is not discussed. Instead, the effects of measurement noise and error on the modal analysis are investigated below.

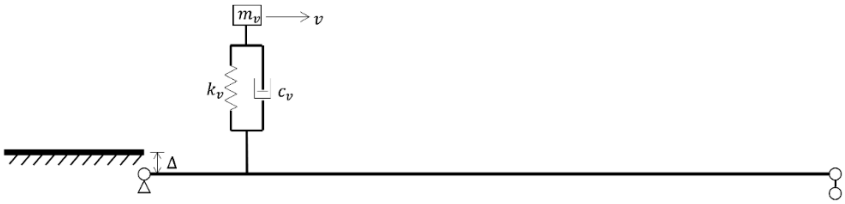

(**a**)

(**b**)

Figure 4. FE model of vehicle passing over a damaged expansion joint: (**a**) illustration; (**b**) ABAQUS.

3.1. Comparison of Results Using Acceleration and Displacement

The impact force can be identified using the time history of displacement, which can be measured directly or calculated by integrating acceleration twice. However, in practice, displacement is usually difficult to measure, and integrating acceleration twice will introduce numerical error. In this subsection, the identification results obtained by displacement and acceleration are compared.

Firstly, the time history of displacement at the midspan obtained directly from the FE model is compared to the calculated displacement by acceleration, which are u_d and u_a in Figure 5. It is observed that u_d shows a slight variation from u_a when the vehicle velocity is no more than 15 m/s, whereas an obvious difference between u_d and u_a can be observed

when the vehicle velocity is as high as 20 m/s. Figure 6 shows the identified impact forces using u_d and u_a. Generally, the identified forces obtained by the proposed method perform well, either using u_d or u_a. These are apparently close to the true value. Moreover, it can be found that when the vehicle velocity is 10 or 15 m/s (Figure 5a,b,d,e), the identified impact forces are almost the same because u_d and u_a are almost the same; however, when the vehicle velocity increases to 20 m/s (Figure 5c,f), the identified forces using u_d are more accurate, whereas the estimated forces by using u_a are lower than expected. This is because the integrated dynamic displacement (u_a) is smaller than the directly obtained dynamic displacement (u_b). The smaller dynamic responses usually correspond to the lower excitation. From Figures 4 and 5, it can be concluded that using u_d to inversely obtain the impact force is more suitable because integrating acceleration introduces unavoidable numerical error, which is calculated as the norm between the vector of integrated dynamic displacement, u_a, and the real dynamic displacement, u_b. However, it should be noted that, in practice, greater differences arise from measuring displacement than acceleration. Considering that the acceleration can be easily measured, only u_a is used in the following study. This is also one of the advantages of the proposed method, which can perform well even if the calculated displacement by acceleration is used; this is validated by the following subsections. Moreover, it should be noted that the proposed method has great efficiency, and the calculation time can be neglected because it is a model-based approach in which only five unknown parameters are included.

3.2. Effect of Measurement Noise

The measurement noise should be always considered in force identification based on dynamic responses. Three levels of noise are investigated herein, which are 1%, 3%, and 5%, because the measurement noise of the vibration signal is usually less than 5% [19,25]. The Gaussian white noise is added to the acceleration directly, and then the displacement can be obtained by integrating the polluted acceleration twice. Using the polluted acceleration, the estimated parameters, including G, A, v, ω, and ξ and the identified maximum impact force, were calculated and are shown in Table 1. Generally, the estimated parameters are not vulnerable to noise and they are quite stable. Even if the noise is as high as 5%, the estimated parameters are almost the same as those obtained using accurate acceleration. This is because the noise is Gaussian white noise, and integration helps to reduce the noise level by performing as a low-pass filter. As a result, the displacements obtained by the acceleration with and without noise show little difference. Therefore, the estimated parameters and identified impact force based on polluted acceleration should be almost the same as those obtained by accurate acceleration.

Table 1. Estimated parameters and identified impact force based on u_a.

Case	Noise Level	G (N) $\times 10^4$	A (N) $\times 10^4$	ω (Hz)	ξ %	v (m/s)	Identified Maximum Force (N) $\times 10^4$	True Maximum Force (N) $\times 10^4$
H05V10	Noise Free	1.22	0.21	3.22	1.57	9.61	1.41	1.40
	Noise 1%	1.22	0.22	3.22	1.58	9.62	1.42	1.40
	Noise 3%	1.21	0.23	3.22	1.52	9.59	1.42	1.40
	Noise 5%	1.24	0.22	3.22	1.67	9.33	1.44	1.40
H05V15	Noise Free	1.19	0.20	3.23	1.42	14.59	1.38	1.40
	Noise 1%	1.19	0.19	3.23	1.41	14.59	1.37	1.40
	Noise 3%	1.19	0.19	3.23	1.45	14.61	1.37	1.40
	Noise 5%	1.18	0.22	3.23	1.39	14.55	1.39	1.40
H05V20	Noise Free	1.12	0.18	3.23	0.47	20.08	1.29	1.40
	Noise 1%	1.12	0.17	3.23	0.46	20.09	1.28	1.40
	Noise 3%	1.12	0.16	3.23	0.42	20.08	1.27	1.40
	Noise 5%	1.11	0.17	3.23	0.50	20.06	1.27	1.40

Table 1. *Cont.*

Case	Noise Level	G (N) $\times 10^4$	A (N) $\times 10^4$	ω (Hz)	ξ %	v (m/s)	Identified Maximum Force (N) $\times 10^4$	True Maximum Force (N) $\times 10^4$
H10V10	Noise Free	1.19	0.43	3.23	2.63	9.77	1.61	1.63
	Noise 1%	1.19	0.44	3.23	2.64	9.72	1.62	1.63
	Noise 3%	1.21	0.45	3.23	2.65	9.88	1.65	1.63
	Noise 5%	1.17	0.45	3.23	2.64	9.63	1.60	1.63
H10V15	Noise Free	1.17	0.45	3.24	2.82	14.75	1.62	1.63
	Noise 1%	1.17	0.43	3.25	2.81	14.77	1.60	1.63
	Noise 3%	1.17	0.45	3.25	2.90	14.76	1.61	1.63
	Noise 5%	1.17	0.44	3.25	2.80	14.76	1.61	1.63
H10V20	Noise Free	1.12	0.42	3.25	2.49	20.09	1.53	1.63
	Noise 1%	1.12	0.41	3.25	2.50	20.09	1.52	1.63
	Noise 3%	1.13	0.42	3.25	2.51	20.09	1.54	1.63
	Noise 5%	1.12	0.41	3.25	2.54	20.05	1.52	1.63

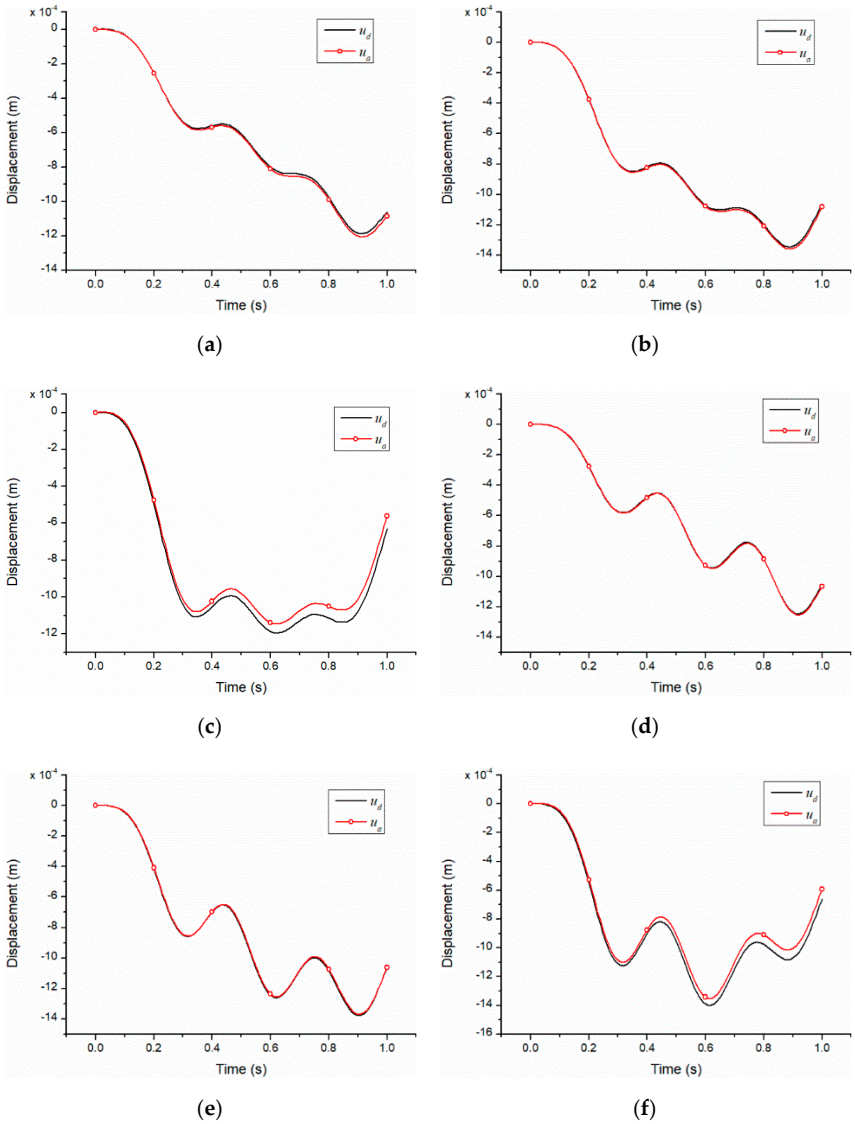

Figure 5. Comparison of directly obtained displacement (u_d) and calculated displacement by integrating acceleration twice (u_a): (**a**) H05V10; (**b**) H05V15; (**c**) H05V20; (**d**) H10V10; (**e**) H10V15; (**f**) H10V20.

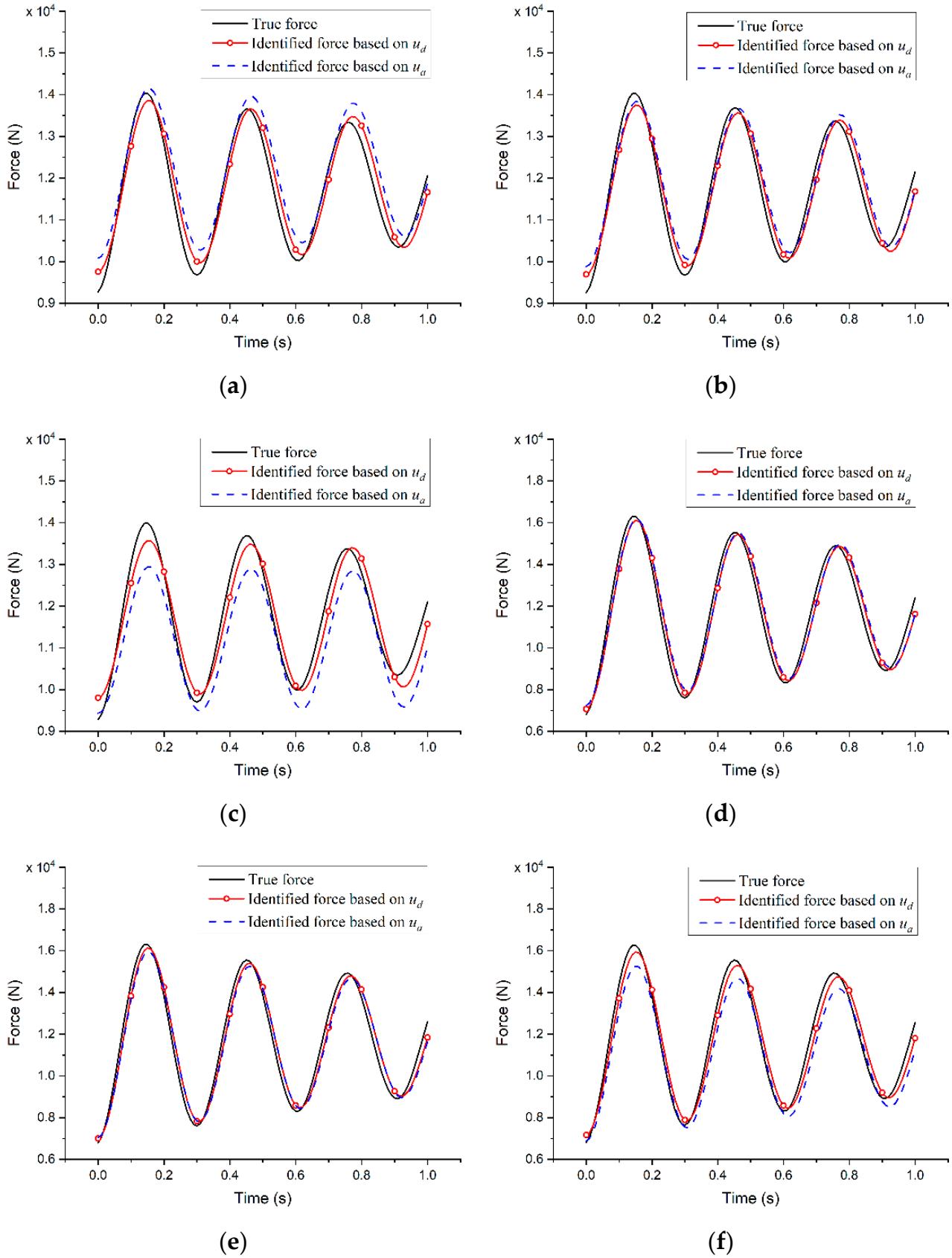

Figure 6. Identified force based on u_d and u_a: (**a**) H05V10; (**b**) H05V15; (**c**) H05V20; (**d**) H10V10; (**e**) H10V15; (**f**) H10V20.

For a better illustration, the identified maximum forces and estimated vehicle velocities for all cases are shown in Figure 7. Figure 7a clearly shows that the noise almost does not influence the identified results. For the cases of H05V20 and H10V20, the identified forces are lower than the true value, because the displacement obtained by integrating the acceleration is lower than the true displacement. It is noteworthy that the integration can help to decrease the white noise, but it cannot reduce the numerical error. Figure 7b shows the estimated vehicle velocities for the six cases. Although the inaccurate displacement results in underestimation of the maximum impact value, the estimated vehicle velocity is quite accurate.

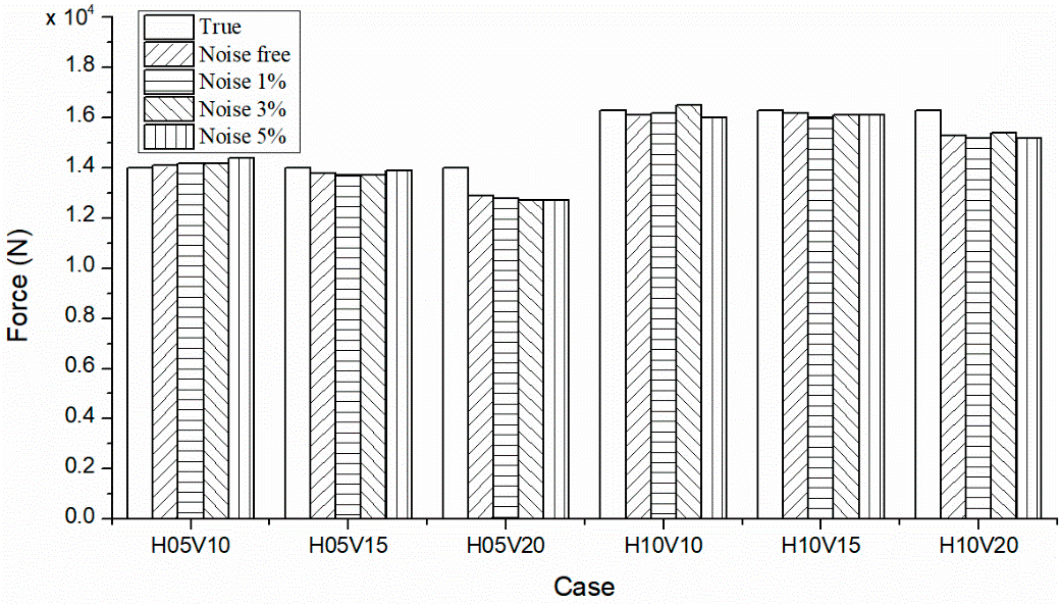

(**a**)

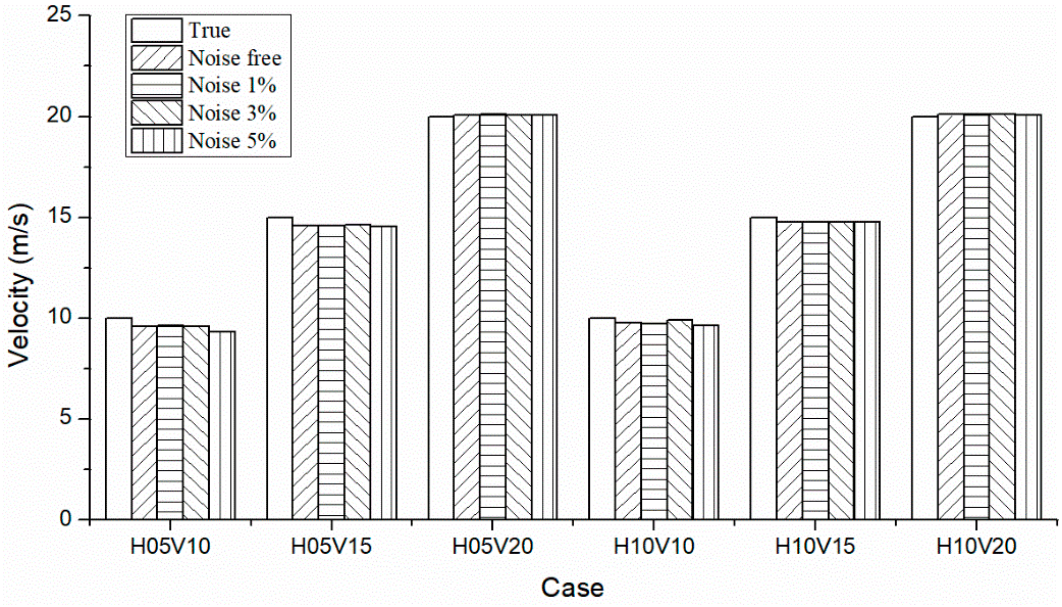

(**b**)

Figure 7. (**a**) Identified maximum impact force and (**b**) estimated velocity based on u_a.

3.3. Effect of Errors of Modal Analysis

The effect of errors of modal analysis is investigated in this subsection because they are usually unavoidable in practice. In this study, it is assumed that the measured frequencies have 1% error and the reconstructed mode shapes have 5% error. By using the first five frequencies and mode shapes with errors, the estimated parameters, including G, A, v, ω, and ξ, and identified maximum impact force, were calculated and are shown in Table 2. Although the error of modal analysis is added, it is found that the proposed method can also give satisfying results.

Table 2. Estimated parameters and identified impact force based on u_a with error of modal analysis.

Case	Noise Level	G (N) $\times 10^4$	A (N) $\times 10^4$	ω (Hz)	ξ %	v (m/s)	Identified Maximum Force (N) $\times 10^4$	True Maximum Force (N) $\times 10^4$
H05V10	Noise Free	1.18	0.15	3.19	1.23	9.37	1.32	1.40
	Noise 1%	1.19	0.15	3.19	1.21	9.39	1.33	1.40
	Noise 3%	1.18	0.14	3.19	1.22	9.35	1.32	1.40
	Noise 5%	1.21	0.15	3.19	1.22	9.10	1.36	1.40
H05V15	Noise Free	1.14	0.14	3.21	0.87	14.48	1.28	1.40
	Noise 1%	1.14	0.14	3.21	0.87	14.48	1.28	1.40
	Noise 3%	1.14	0.16	3.21	0.86	14.51	1.30	1.40
	Noise 5%	1.13	0.14	3.21	0.85	14.44	1.27	1.40
H05V20	Noise Free	1.07	0.15	3.23	0.18	19.97	1.22	1.40
	Noise 1%	1.07	0.14	3.23	0.18	19.96	1.21	1.40
	Noise 3%	1.07	0.14	3.23	0.17	19.95	1.22	1.40
	Noise 5%	1.06	0.13	3.23	0.18	19.94	1.19	1.40
H10V10	Noise Free	1.16	0.38	3.22	2.12	9.55	1.54	1.63
	Noise 1%	1.16	0.39	3.23	2.13	9.49	1.54	1.63
	Noise 3%	1.18	0.41	3.22	2.13	9.66	1.58	1.63
	Noise 5%	1.13	0.40	3.22	2.14	9.40	1.53	1.63
H10V15	Noise Free	1.12	0.38	3.24	2.31	14.66	1.50	1.63
	Noise 1%	1.12	0.38	3.24	2.30	14.69	1.50	1.63
	Noise 3%	1.12	0.39	3.24	2.39	14.67	1.51	1.63
	Noise 5%	1.12	0.37	3.24	2.30	14.67	1.49	1.63
H10V20	Noise Free	1.07	0.36	3.24	1.91	20.05	1.42	1.63
	Noise 1%	1.07	0.35	3.24	1.92	20.05	1.42	1.63
	Noise 3%	1.08	0.37	3.24	1.92	20.05	1.44	1.63
	Noise 5%	1.07	0.37	3.24	1.97	20.01	1.44	1.63

A similar observation can be obtained, in which the noise almost does not influence the estimated parameters and identified impact forces. However, it is seen from Figure 8 that the identified maximum forces are less accurate compared to those without the error of modal analysis, which means that the error of modal analysis influences the identified maximum impact forces more significantly than the measurement noise of acceleration. Figure 9 shows the estimated vehicle velocities for these six cases. It is found that the estimated velocities are less sensitive to the error of modal analysis than the identified maximum values. For some cases (H05V20 and H10V20), the estimated velocities with the error of modal analysis are even more accurate.

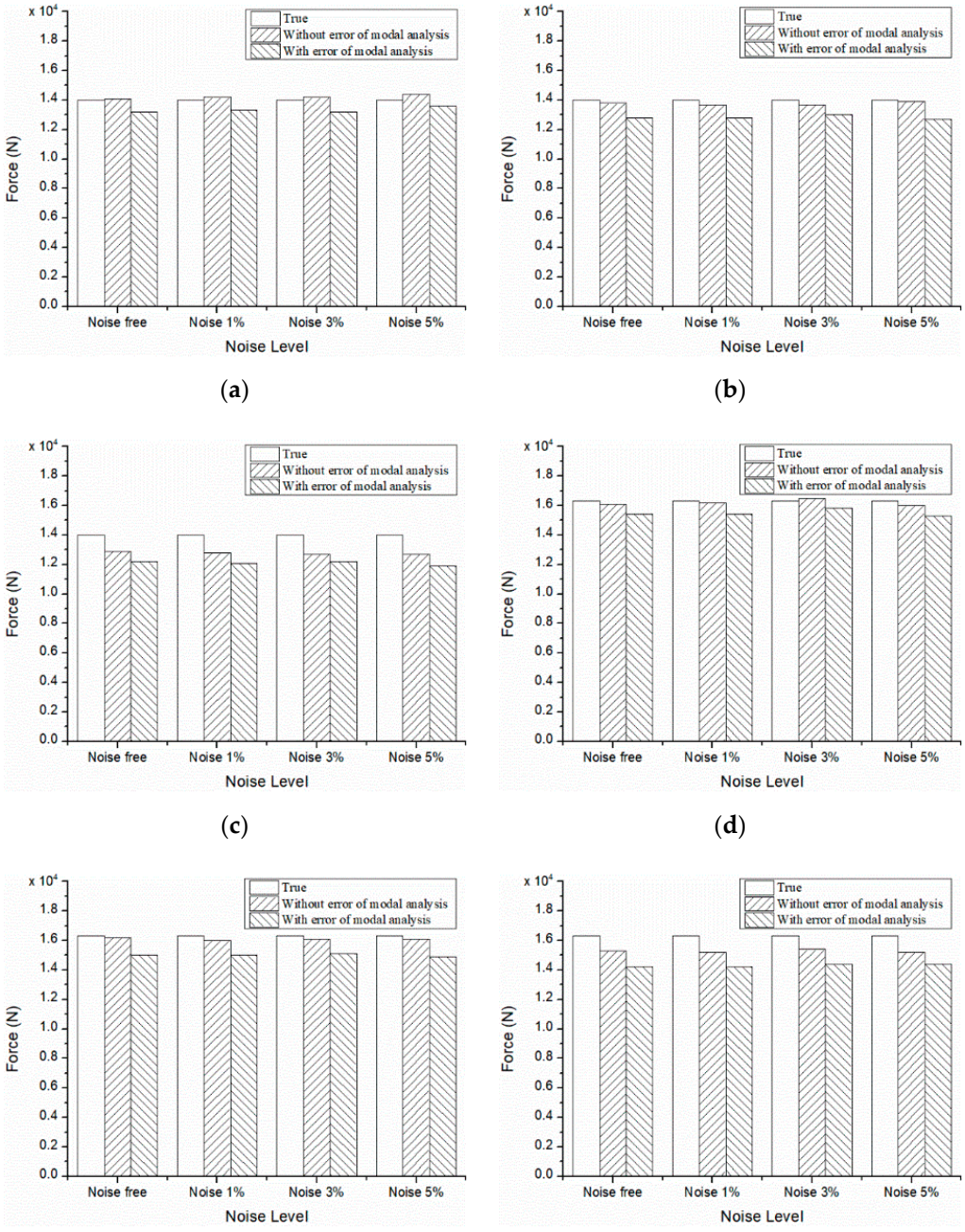

Figure 8. Comparison of estimated maximum force with and without error of modal analysis: (**a**) H05V10; (**b**) H05V15; (**c**) H05V20; (**d**) H10V10; (**e**) H10V15; (**f**) H10V20.

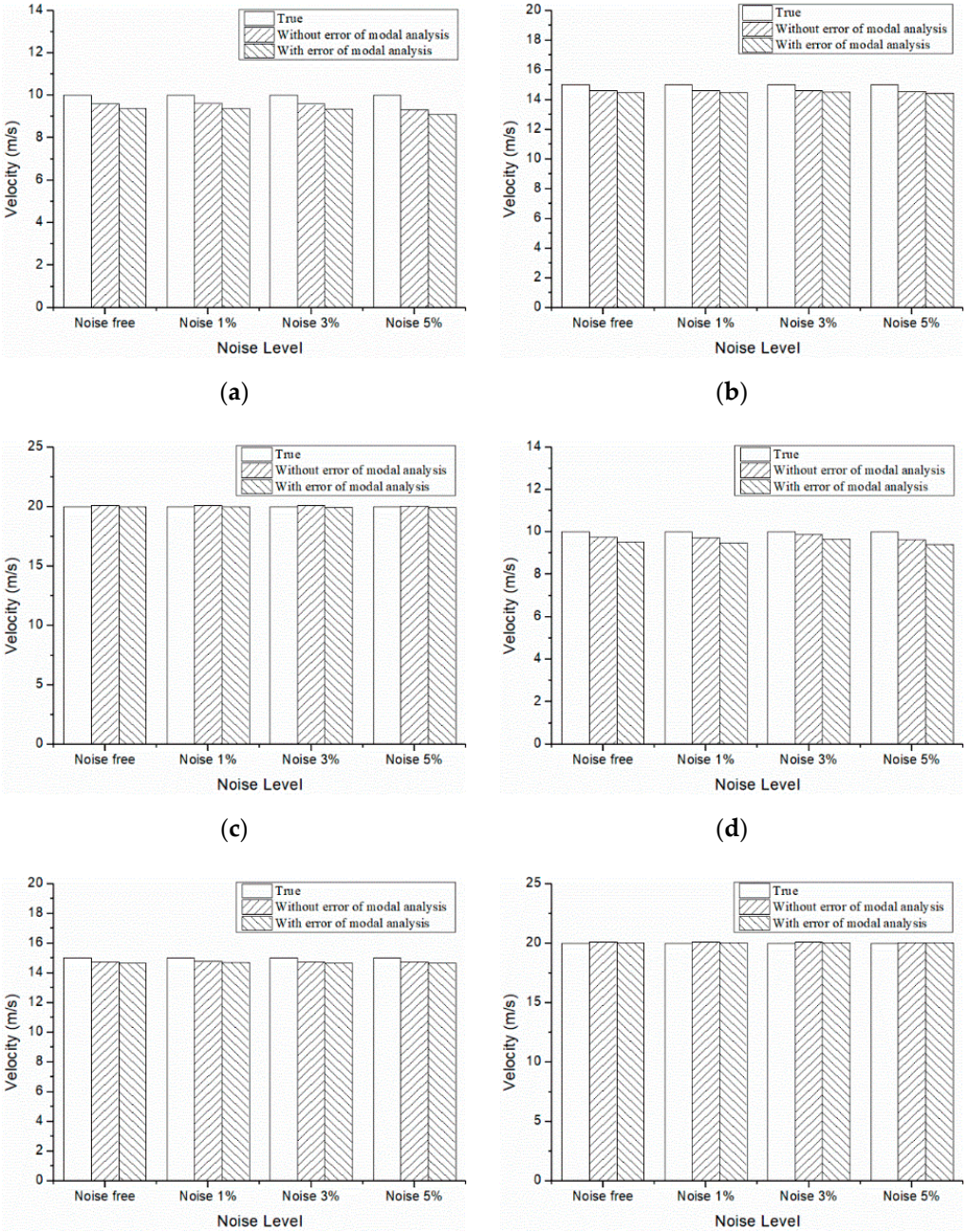

Figure 9. Comparison of estimated vehicle velocity with and without error of modal analysis: (**a**) H05V10; (**b**) H05V15; (**c**) H05V20; (**d**) H10V10; (**e**) H10V15; (**f**) H10V20.

4. Conclusions

This study proposes a model-based method to identify the vehicle impact on bridges due to a damaged expansion joint, in which the impact force is simulated as an exponentially damped sine function. The unknown parameters can be determined easily by solving a typical optimization problem based on the conjugate direction method. It can be implemented more conveniently than general basis function-based methods because it has only five unknown parameters. Numerical simulations were conducted to validate the proposed method and investigate the effect of different factors on the proposed method. The findings can be concluded as follows:

(1) The proposed method can identify the dynamic impact accurately when the displacement of the bridge midspan is obtained by integrating the acceleration twice, even if it has inevitable numerical errors.
(2) When the noise level is in the range of 1% to 5%, the proposed method can still perform well, although the identification results are slightly less accurate with the increase in measurement noise level.
(3) The error of modal analysis greatly affects the proposed method, especially for identification of maximum force, and therefore, the mode shapes of the bridge should be measured accurately to ensure the performance of the proposed method.

Finally, it should be noted that the proposed method mainly focuses on the identification of a single dynamic impact, and may fail if two vehicles pass the same damaged expansion joint within a very short time interval. Hence, identification of multiple dynamic impacts within a short time interval should be investigated in the future.

Author Contributions: Methodology, J.G., J.L.; Software, X.Z.; Supervision, J.G.; Writing—original draft, J.G., X.Z.; Writing—review & editing, J.L. All authors have read and agreed to the published version of the manuscript.

Funding: This research was funded by Natural Science Foundation of China (U2005216), Science and Technology Research and Development Plan of China Railway Group Limited (2020-Key-11), Natural Science Foundation of Fujian (2020J01010).

Institutional Review Board Statement: Not applicable.

Informed Consent Statement: Not applicable.

Data Availability Statement: Not applicable.

Acknowledgments: We are grateful to the following agencies for their supports in this study: Natural Science Foundation of China (U2005216), Science and Technology Research and Development Plan of China Railway Group Limited (2020-Key-11), Natural Science Foundation of Fujian (2020J01010).

Conflicts of Interest: The authors declare no conflict of interest.

References

1. AASHTO. *LRFD Bridge Design Specifications*; AASHTO: Washington, DC, USA, 2010.
2. Deng, L.; Yu, Y.; Zou, Q.; Cai, C.S. State-of-the-Art Review of Dynamic Impact Factors of Highway Bridges. *J. Bridg. Eng.* **2015**, *20*, 04014080. [CrossRef]
3. Yang, Y.; Zhang, Y.; Tan, X. Review on Vibration-Based Structural Health Monitoring Techniques and Technical Codes. *Symmetry* **2021**, *13*, 1998. [CrossRef]
4. Cai, C.; Shi, X.; Araujo, M.; Chen, S. Effect of approach span condition on vehicle-induced dynamic response of slab-on-girder road bridges. *Eng. Struct.* **2007**, *29*, 3210–3226. [CrossRef]
5. Shi, X.; Cai, C.S.; Chen, S. Vehicle Induced Dynamic Behavior of Short-Span Slab Bridges Considering Effect of Approach Slab Condition. *J. Bridg. Eng.* **2008**, *13*, 83–92. [CrossRef]
6. Deng, L.; Yan, W.; Zhu, Q. Vehicle Impact on the Deck Slab of Concrete Box-Girder Bridges due to Damaged Expansion Joints. *J. Bridg. Eng.* **2015**, *21*, 06015006. [CrossRef]
7. Ding, Y.; Zhuge, P.; Xie, X.; Li, H.; Huang, J.Y. Numerical analysis of dynamic load in bridge-head bumping considering the contact length between tire and road. *J. Vib. Shock* **2013**, *32*, 28–34. [CrossRef]
8. Ding, Y.; Zhang, W.; Au, F.T.K. Effect of dynamic impact at modular bridge expansion joints on bridge design. *Eng. Struct.* **2016**, *127*, 645–662. [CrossRef]
9. Xie, X.; Wu, D.Y.; Wang, J.F.; Zhang, S.Q.; Zhou, Y.J. Dynamical behavior of steel box girder bridges due to vehicle-induced vibration at expansion joint. *J. Zhejiang Univ. (Eng. Sci.)* **2009**, *10*, 029. [CrossRef]
10. Do, T.V.; Pham, T.M.; Hao, H. Impact force profile and failure classification of reinforced concrete bridge columns against vehicle impact. *Eng. Struct.* **2019**, *183*, 443–458. [CrossRef]
11. Ma, H.; Cao, Z.; Shi, X.; Zhou, J. Dynamic Amplification Factor of Shear Force on Bridge Columns under Impact Load. *Shock Vib.* **2019**, *2019*, 1–14. [CrossRef]
12. Wu, M.; Jin, L.; Du, X. Dynamic response analysis of bridge precast segment piers under vehicle collision. *Eng. Fail. Anal.* **2021**, *124*, 105363. [CrossRef]
13. Zhu, X.Q.; Law, S.S. Orthogonal function in moving loads identification on a multi-span bridge. *J. Sound Vib.* **2001**, *245*, 329–345. [CrossRef]

14. Wu, S.; Law, S. Vehicle axle load identification on bridge deck with irregular road surface profile. *Eng. Struct.* **2011**, *33*, 591–601. [CrossRef]
15. Law, S.S.; Chan, T.H.T.; Zhu, Q.X.; Zeng, Q.H.; Zhu, X. Regularization in Moving Force Identification. *J. Eng. Mech.* **2001**, *127*, 136–148. [CrossRef]
16. Au, F.; Jiang, R.; Cheung, Y. Parameter identification of vehicles moving on continuous bridges. *J. Sound Vib.* **2004**, *269*, 91–111. [CrossRef]
17. Deng, L.; Cai, C.S. Identification of parameters of vehicles moving on bridges. *Eng. Struct.* **2009**, *31*, 2474–2485. [CrossRef]
18. Vosoughi, A.R.; Anjabin, N. Dynamic moving load identification of laminated composite beams using a hybrid FE-TMDQ-GAs method. *Inverse Probl. Sci. Eng.* **2017**, *25*, 1639–1652. [CrossRef]
19. Gunawan, F.E. Impact force reconstruction using the regularized Wiener filter method. *Inverse Probl. Sci. Eng.* **2016**, *24*, 1107–1132. [CrossRef]
20. Li, Q.; Lu, Q. Impact localization and identification under a constrained optimization scheme. *J. Sound Vib.* **2016**, *366*, 133–148. [CrossRef]
21. Gupta, D.K.; Dhingra, A.K. A reduced modal parameter based algorithm to estimate excitation forces from optimally placed accelerometers. *Inverse Probl. Sci. Eng.* **2017**, *25*, 397–417. [CrossRef]
22. Liu, Y.; Shepard, W.S. An improved method for the reconstruction of a distributed force acting on a vibrating structure. *J. Sound Vib.* **2006**, *291*, 369–387. [CrossRef]
23. Gunawan, F.E.; Homma, H. A solution of the ill-posed impact-force inverse problems by the weighted least squares method. *J. Solid Mech. Mater. Eng.* **2008**, *2*, 188–198. [CrossRef]
24. Gunawan, F.E.; Homma, H. Impact-force estimation by quadratic spline approximation. *J. Solid Mech. Mater. Eng.* **2008**, *2*, 1092–1103. [CrossRef]
25. Gunawan, F.E.; Homma, H.; Kanto, Y. Two-step B-splines regularization method for solving an ill-posed problem of impact-force reconstruction. *J. Sound Vib.* **2006**, *297*, 200–214. [CrossRef]
26. Qiao, B.; Zhang, X.; Luo, X.; Chen, X. A force identification method using cubic B-spline scaling functions. *J. Sound Vib.* **2015**, *337*, 28–44. [CrossRef]
27. Li, Z.; Feng, Z.; Chu, F. A load identification method based on wavelet multi-resolution analysis. *J. Sound Vib.* **2014**, *333*, 381–391. [CrossRef]
28. Xu, X.; Ou, J. Force identification of dynamic systems using virtual work principle. *J. Sound Vib.* **2015**, *337*, 71–94. [CrossRef]
29. Pourzeynali, S.; Zhu, X.; Zadeh, A.G.; Rashidi, M.; Samali, B. Comprehensive Study of Moving Load Identification on Bridge Structures Using the Explicit Form of Newmark-β Method: Numerical and Experimental Studies. *Remote Sens.* **2021**, *13*, 2291. [CrossRef]
30. Wang, H.; Nagayama, T.; Su, D. Static and dynamic vehicle load identification with lane detection from measured bridge acceleration and inclination responses. *Struct. Control Health Monit.* **2021**, *28*, e2823. [CrossRef]
31. Zhang, Y.; Xie, J.; Peng, J.; Li, H.; Huang, Y. A deep neural network-based vehicle re-identification method for bridge load monitoring. *Adv. Struct. Eng.* **2021**, *24*, 3691–3706. [CrossRef]
32. Xia, Y.; Lei, X.; Wang, P.; Sun, L. Artificial Intelligence Based Structural Assessment for Regional Short- and Medium-Span Concrete Beam Bridges with Inspection Information. *Remote Sens.* **2021**, *13*, 3687. [CrossRef]
33. Yang, Y.; Cheng, Q.; Zhu, Y.; Wang, L.; Jin, R. Feasibility Study of Tractor-Test Vehicle Technique for Practical Structural Condition Assessment of Beam-Like Bridge Deck. *Remote Sens.* **2020**, *12*, 114. [CrossRef]
34. Yang, Y.; Lu, H.; Tan, X.; Chai, H.K.; Wang, R.; Zhang, Y. Fundamental mode shape estimation and element stiffness evaluation of girder bridges by using passing tractor-trailers. *Mech. Syst. Signal Process.* **2021**, *169*, 108746. [CrossRef]
35. Andrei, N. Standard conjugate gradient methods, Nonlinear conjugate gradient methods for unconstrained optimization. In *Springer Optimization and Its Application*; Springer: Berlin/Heidelberg, Germany, 2020; pp. 125–160. [CrossRef]